



# Fermented and Germinated Processing Improved the Protective Effects of Foxtail Millet Whole Grain Against Dextran Sulfate Sodium-Induced Acute Ulcerative Colitis and Gut Microbiota Dysbiosis in C57BL/6 Mice

## OPEN ACCESS

### Edited by:

Jinkai Zheng,  
Chinese Academy of Agricultural  
Sciences (CAAS), China

### Reviewed by:

Ashok Kumar Pandurangan,  
B. S. Abdur Rahman Crescent  
Institute of Science and  
Technology, India  
Guodong Zhang,  
University of Massachusetts Amherst,  
United States  
Parmanand Malvi,  
Yale University, United States  
Zhigang Liu,  
Northwest A and F University, China

### \*Correspondence:

Wei Liu  
980701611@qq.com  
Lingfei Li  
lingfeili@163.com

### Specialty section:

This article was submitted to  
Food Chemistry,  
a section of the journal  
Frontiers in Nutrition

**Received:** 14 April 2021

**Accepted:** 07 July 2021

**Published:** 29 July 2021

### Citation:

Zhang Y, Liu W, Zhang D, Yang Y,  
Wang X and Li L (2021) Fermented  
and Germinated Processing Improved  
the Protective Effects of Foxtail Millet  
Whole Grain Against Dextran Sulfate  
Sodium-Induced Acute Ulcerative  
Colitis and Gut Microbiota Dysbiosis in  
C57BL/6 Mice. *Front. Nutr.* 8:694936.  
doi: 10.3389/fnut.2021.694936

Yuhan Zhang<sup>1,2,3</sup>, Wei Liu<sup>2\*</sup>, Di Zhang<sup>3</sup>, Yanbing Yang<sup>2</sup>, Xianshu Wang<sup>2</sup> and Lingfei Li<sup>1\*</sup>

<sup>1</sup> College of Food Science and Technology, Yunnan Agricultural University, Kunming, China, <sup>2</sup> Institute of Agro-Food Science and Technology, Shandong Academy of Agricultural Sciences, Jinan, China, <sup>3</sup> Qilu Hospital, Shandong University, Jinan, China

This study investigated the effects of foxtail millet whole grain flours obtained through different processing methods on alleviating symptoms and gut microbiota dysbiosis in a dextran sulfate sodium (DSS)-induced murine colitis model. Sixty C57BL/6 mice were divided into six groups ( $n = 10$  in each group), including one control group (CTRL) without DSS treatment and five DSS-treated groups receiving one of the following diets: AIN-93M standard diet (93MD), whole grain foxtail millet flour (FM), fermented (F-FM), germinated (G-FM), and fermented-germinated foxtail millet flour (FG-FM). A comparison of the disease activity index (DAI) demonstrated that foxtail millet whole grain-based diets could alleviate the symptoms of enteritis to varying degrees. In addition, 16S rRNA gene sequencing revealed that FG-FM almost completely alleviated DSS-induced dysbiosis. Mice on the FG-FM diet also had the lowest plasma IL-6 levels and *claudin2* expression levels in the colon, indicating reduced systemic inflammation and improved gut barrier function. This study suggested that foxtail millet whole grain is an attractive choice for the intervention of IBD and gut microbiota dysbiosis, and its prebiotic properties are highly affected by the processing methods.

**Keywords:** foxtail millet, fermentation, germination, gut microbiota, inflammatory bowel disease, mouse colitis model

## INTRODUCTION

Inflammatory bowel disease (IBD) is a chronic and incurable inflammatory disease that has two major entities: Crohn's disease (CD) and ulcerative colitis (UC) (1). Patients with IBD suffer from multiple clinical symptoms, including abdominal pain, diarrhea, blood in stools, and weight loss, as well as having a higher risk of developing colorectal carcinoma (CRC) (2). In this century, IBD has become a global health concern because of its high disease burden in Western countries and increasing prevalence in newly industrialized countries in Asia, Africa, and South America (3).

At present, IBD is widely accepted to be a multifactor disease driven by complex interactions among genetics, environmental factors, and the host immune system (4). The precise etiology of IBD is still unclear, which is a major problem for the prevention and medical therapy of IBD (5).

The gut microbiota is a collective term for microorganisms that live in the intestine of humans and other animals. The gut microbiota is primarily made up of bacteria, but it also includes viruses, archaea, and fungi inhabiting the gastrointestinal tract (6). It is the largest independent organ of the human body, performing indispensable functions such as digestion, absorption, metabolism, and immunity (7). There has been increasing evidence indicating that dysbiosis of the gut microbiota, which is usually manifested as a decrease in gut microbial diversity or a shift in the balance between commensal and potentially pathogenic bacteria (1), plays an important role in IBD and IBD-associated CRC (6). The reduction in gut microbial diversity, as well as differences in the composition of gut microbiota between IBD patients and healthy controls, have previously been demonstrated (8). For instance, several species of the phylum *Proteobacteria* have been reported as microbial signatures for gut microbiota in IBD patients (9). The most studied member of the *Proteobacteria*, *Escherichia coli*, was found to be excessively proliferated in IBD patients, playing a non-eligible role in the development of IBD (10). Along with an increase in the relative abundance of species from the phylum *Proteobacteria*, the abundance of the phyla *Firmicutes* and *Bacteroidetes*, which are the dominant phyla in the gut microbiota of healthy individuals, was significantly decreased in IBD patients (11).

The key factors for the pathogenesis of IBD have been highlighted. Therefore, the gut microbiota has emerged as a promising new target for the prevention and clinical treatment of IBD. In clinical practice, the application of fecal microbiota transplantation (FMT) has been proven to be effective in alleviating clinical symptoms in IBD patients (12). However, the potential hazards of FMT remain controversial, making the possibility of its widespread application unclear (13). Probiotic therapy has also been shown to be effective in both murine colitis models and IBD patients (14). In addition, due to the direct impact on the gut microbiota (15), dietary ingredients can also be used as promising strategies for the prevention and therapy of IBD due to their direct impact on the gut microbiota (15). Several food polyphenols and specific carbohydrates, for example, are effective in relieving the clinical symptoms of IBD (16, 17).

Cereals are at the bottom of the nutrition pyramid and make up a large percentage of the daily diet. Foxtail millet (*Setaria italica* Beauv.) is an old staple crop in Europe and Asia and is still one of the main food crops in northern China (18). Foxtail millet has superior nutritional properties among cereals, containing high amounts of proteins, minerals, and vitamins (19). In addition to being a daily nutritional source, small millets, including foxtail millet, have anti-inflammatory properties and can therefore be used for the prevention of related chronic diseases, such as atherosclerosis and diabetes (20, 21). Along with its superior nutritional properties and documented anti-inflammatory function, foxtail millet is also rich in non-nutrient

prebiotics, such as polyphenols and dietary fibers (22), suggesting its possible positive effects on the gut microbiota and IBD. Bond polyphenols and peroxidase of foxtail millet bran have also been reported to inhibit colitis-induced carcinogenesis in a mouse model (23, 24).

In daily life, the foxtail millet is usually peeled and refined rather than the whole grain. The dehulling process results in a significant decrease in antinutrients and an increase in the bioavailability of foxtail millet, reducing the burden on the digestive system (19). However, the cereal bran, which is lost during the peeling process, contains abundant prebiotics that can effectively promote the growth of probiotics, modulate the bacterial composition of gut microbiota, and increase the production of short-chain fatty acids (SCFAs) (25). In addition to dehulling, germination and fermentation have also been reported to decrease the contents of anti-nutrients and improve the digestibility of whole grains, such as millets (26). Germination induces a significant increase in free amino acids, as well as significant beneficial effects on the availability of polyphenolic components, minerals, and  $\gamma$ -aminobutyrate (GABA) in foxtail millet (27, 28). On the other hand, the fermentation process causes the degradation of cellulose and hemicellulose in the cereal bran, resulting in the formation of more porous and loose structures and polysaccharides, which significantly improves the digestibility and prebiotic properties of foxtail millet (26).

In order to develop cost-effective dietary strategies for the prevention of IBD, this study investigated the alleviation of gut microbiota dysbiosis and the reduction in the symptoms of DSS-induced murine colitis models using foxtail millet flours obtained through different processing methods. Based on the hypothesis that different pretreatment methods will affect the function of millet in the prevention of colon colitis, four foxtail millet whole-grain cereal flours were studied: foxtail millet whole grain flour (FM), fermented foxtail millet whole grain flour (F-FM), germinated foxtail millet whole grain flour (G-FM), and fermented-germinated foxtail millet flour (FG-FM). This study used a traditional staple food in daily life as a dietary intervention for IBD to provide a new perspective for the prevention and treatment of IBD.

## MATERIALS AND METHODS

### Preparation of Foxtail Millet Cereal Flours and Animal Diets

The foxtail millet used in this study was provided by the Crop Institute, Shandong Academy of Agricultural Science (Jinan, China). Both FM and G-FM were prepared using foxtail millet whole grains and germinated foxtail millet whole grains, respectively. F-FM and FG-FM were prepared by fermenting foxtail millet whole grains or germinated foxtail millet whole grains by fermentation using *Lactobacillus plantarum* NBRC 15,891 (29), respectively. The following are the preparation details:

**FM:** The foxtail millet whole grain seeds were ground and screened using an 80-mesh sieve to prepare the foxtail millet whole grain flour (FM).

**F-FM:** The FM flour was mixed with tap water (1:3) and heated for 10 minutes in a  $75\pm 5^\circ\text{C}$  water bath to gelatinize the starch. After that, it was inoculated with *L. plantarum* NBRC 15,891 at a concentration of  $10^6$  CFU per 100 g FM flour and incubated at  $37^\circ\text{C}$  until the pH dropped to  $4.0 \pm 0.2$ . The resulting slurry was dried at  $55^\circ\text{C}$ , ground and screened using an 80-mesh sieve to produce fermented polished foxtail millet flour (F-PFM).

**G-FM:** The germinated foxtail millet was prepared as described previously (30). The foxtail millet seeds were soaked in tap water overnight at room temperature. After draining the water, the seeds were spread out on a moist muslin cloth and covered with moist absorbent gauze. The seeds were left to sprout at room temperature for 48 h. After sprouting, the germinated seeds were dried at  $55^\circ\text{C}$  before being ground and screened using an 80-mesh sieve to prepare the germinated whole-grain foxtail millet flour (G-FM).

**FG-FM:** FG-FM flour was prepared using G-FM flour following the same preparation procedure that was used for F-FM.

The contents of starch, total proteins, crude fats, ashes, dietary fibers, and the moisture of cereal flours are provided in (Supplementary Table 1). Cereal flour-based animal diets were designed based on the AIN-93M standard rodent formula. The foxtail millet test diets contained 50% cereal flours, with the remaining 50% supplemented with standard nutrients according to the AIN-93M formula. The animal diets were prepared by Nantong Troffe Technology Co., Ltd. (Jiangsu, China). The detailed compositions of the experimental diets are provided in (Supplementary Table 2).

## Detection of the Main Compounds in Foxtail Millet Cereal Flours With LC/MS Analysis

The detailed method of sample preparation has been previously described (31). A total of 50 mg sample was weighted, and a 1,000  $\mu\text{L}$  extract solution (methanol: water = 3:1 with isotopically labeled internal standard mixture) was added. The samples were then homogenized at 35 Hz for 4 min and sonicated for 5 min in an ice-water bath. Both the homogenization and sonication cycles were repeated three times. After that, the samples were incubated for 1 h at  $-40^\circ\text{C}$  and centrifuged at 12,000 rpm for 15 min at  $4^\circ\text{C}$ . The resulting supernatant was transferred to a new glass vial for analysis. The quality control (QC) sample was prepared by mixing an equal aliquot of the supernatants from each sample.

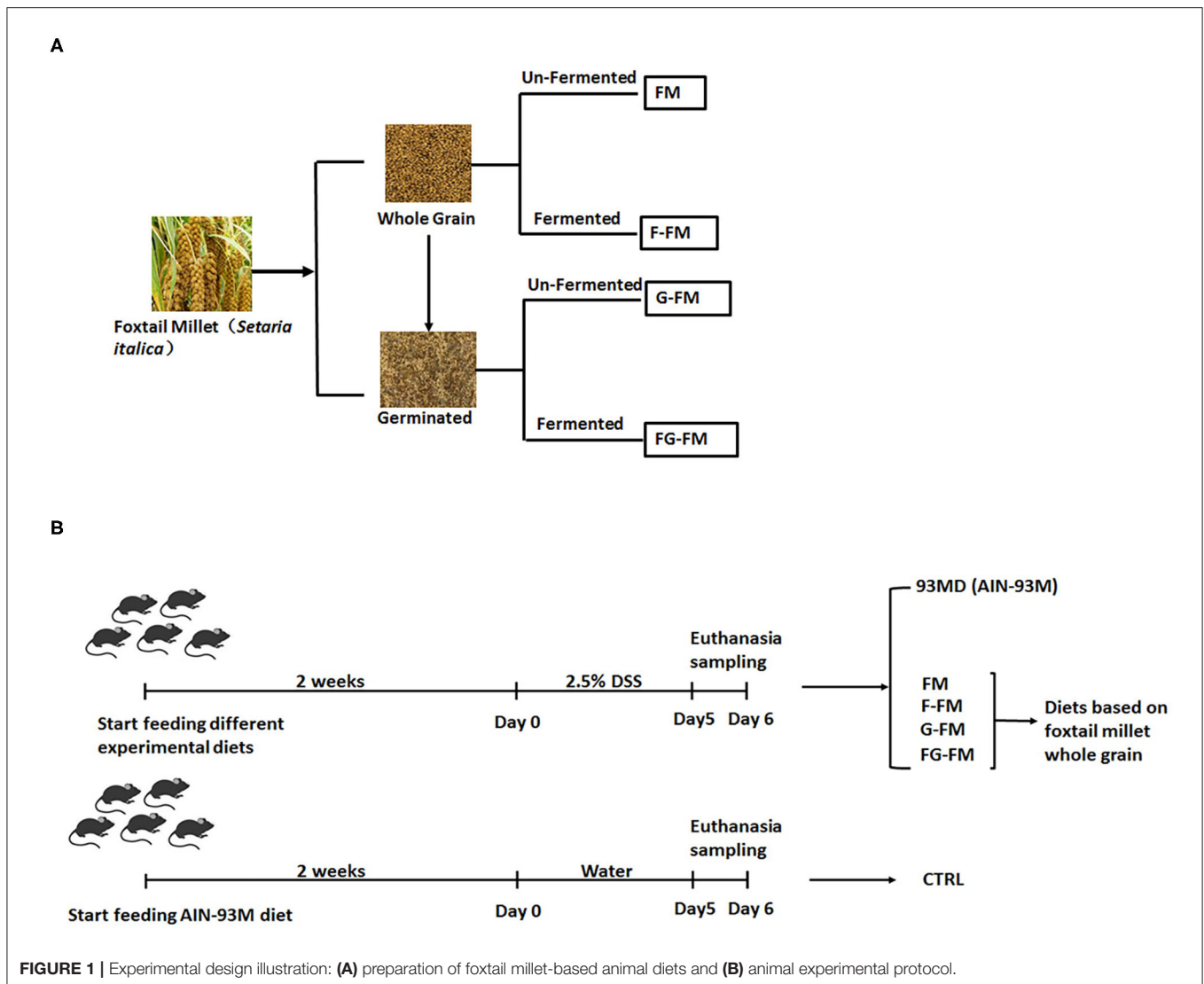
The LC-MS/MS analyses were performed using a UHPLC system (Vanquish, Thermo Fisher Scientific) with a UPLC HSS T3 column ( $2.1 \times 100$  mm,  $1.8 \mu\text{m}$ ) coupled to a Q Exactive HFX mass spectrometer (Orbitrap MS, Thermo). The mobile phase consisted of 5 mmol/L ammonium acetate and 5 mmol/L acetic acid in water (A) and acetonitrile (B). The auto-sampler temperature was  $4^\circ\text{C}$ , and the injection volume was 3  $\mu\text{L}$ . The QE HFX mass spectrometer was used to acquire MS/MS spectra using the information-dependent acquisition (IDA) mode in

the control of the acquisition software (Xcalibur, Thermo). In this mode, the acquisition software continuously evaluates the full scan MS spectrum. The following ESI source parameters were used: sheath gas flow rate at 30 Arb, Aux gas flow rate at 10 Arb, capillary temperature at  $350^\circ\text{C}$ , full MS resolution at 60,000, MS/MS resolution at 7,500, collision energy at 10/30/60 in NCE mode, and spray Voltage at 4.0 kV (positive) or  $-3.8$  kV (negative), respectively. The resulting raw data were converted to the mzXML format using ProteoWizard and processed with an in-house program, which was developed using R and based on XCMS, for peak detection, extraction, alignment, and integration. Then, metabolite annotation was performed using an in-house MS2 database (BiotreeDB). The cutoff for annotation was set at 0.3.

## Animals Experiments Design

Preparation of foxtail millet-based animal diets and animal experimental protocols are shown in Figures 1A,B. Sixty male C57BL/6 mice (6 weeks old) were purchased from the Model Animal Research Center of Nanjing University (Nanjing, China) and housed in a specific pathogen-free facility with ad libitum access to food and water. After two weeks of acclimation, the mice were randomly assigned to one of the following six experimental diet groups ( $n = 10$  per diet, 5 mice per cage): CTRL group (control group; mice fed an AIN-93M standard diet, without being exposed to DSS); 93MD group (mice fed an AIN-93M standard diet); FM group (mice fed an FM flour diet); F-FM group (mice fed an F-FM flour diet); G-FM group (mice fed a G-FM flour diet) and FG-FM group (mice fed an FG-FM flour diet).

After one week of experimental diet supplementation, all mice (except mice from the CTRL group) were exposed to DSS treatment (molecular weight 36–50 kDa; MP Biomedicals) in their drinking water (2.5%) for five consecutive days, with the first day of DSS treatment was designated as day 0. The DSS solution was freshly prepared and replaced every day. After five days of DSS treatments, the mice were anesthetized with isoflurane, and blood was collected with a capillary tube containing 1% heparin sodium solution by orbital puncture. Following that, the blood was centrifuged at 6,000 rpm for 10 minutes to obtain plasma. After the mice were sacrificed by cervical dislocation, their abdomens were opened and cecal contents were collected, snap-frozen in liquid nitrogen, then stored at  $-80^\circ\text{C}$  for further analysis. The length of the mouse colon was measured from the colon-cecal junction to the anus. A 2-cm section of the mouse colon was fixed for histological analysis, and then the rest was collected and snap-frozen in liquid nitrogen for further analysis. The spleen and liver weights of the mice were recorded. The animals were cared for according to the Guide for P.R. China Legislation on the Use and Care of Laboratory Animals. All experimental procedures were approved by the Animal Care and Use Ethics Committee of the Institute of Agro-food Science and Technology at Shandong Academy of Agricultural Sciences (Jinan, China) (Approval ID: SDAA-IAFST-2018003).



## Evaluation of Disease Activity Index (DAI)

During induction, disease progression was evaluated by recording body weight, stool characteristics and rectal bleeding every day. The DAI was determined by combining the measured scores of body weight (0–4), stool consistency (0–3), and rectal bleeding (0–3) as previously described (32, 33). The measured score ranges were as follows: body weight loss (0 =  $\leq 1\%$ ; 1 = 1–5%; 2 = 5–10%; 3 = 10–20%; and 4 =  $>20\%$ ), stool consistency (0 = normal; 1 = soft stools; 2 = loose stools; and 3 = diarrhea), and rectal bleeding (0 = negative hemocult; 1 = hemocult; 3 = traces of blood; and 4 = visible rectal bleeding).

## Histopathological Scores

For histopathological observations, the colon tissues were fixed in 10% formalin for more than 48 h, sectioned at 5  $\mu\text{m}$ , and stained

with hematoxylin-eosin. Eight fields were randomly selected in each section and were scored for colonic epithelial damage (0–6), inflammatory infiltrate in the mucosa (0–3), submucosa (0–2) and muscularis/serosa (0–1) as previously described (34). The given scores were described as follows: colonic epithelial damage (0 = normal; 1 = hyperproliferation, irregular crypts, and goblet cell loss; 2 = 10–50% crypt loss; 3 = 50–90% crypt loss; 4 = complete crypt loss, surface epithelium intact; 5 = small- to medium-sized ulcer,  $<10$  crypt width; 6 = large-scale ulcer,  $<10$  crypt width), inflammatory infiltrate in the mucosa (0 = normal; 1 = mild; 2 = modest; 3 = severe), submucosa (0 = normal; 1 = mild to modest; 2 = severe), and muscularis/serosa (0 = normal; 1 = moderate to severe). The average scores of eight randomly selected fields for all four individual scores were added, which resulted in a total scoring range of 0–12 per colon.

## Analysis of Gut Microbiota Using 16S rRNA Gene Sequencing

The 16S rRNA gene sequencing method has been previously described (33). Total bacterial DNA was extracted from frozen cecal content, the V3-V4 region of the 16S rRNA gene was amplified, and a DNA library was constructed. Paired-end sequencing with a read length of  $2 \times 150$  bp was performed using the Illumina HiSeq platform (Illumina, Inc., San Diego, California). The demultiplexed paired-end reads were joined using the FLASH v1.2.7 software (35), quality filtered (36), and the chimerism was removed (37). The resulting tags were then assigned to OTUs (38) with a 97% threshold of pairwise identity and aligned using the Silva reference database (Release 128, <http://www.arb-silva.de>) (39).

## Quantification of Inflammatory Cytokines in Mouse Plasma

Mouse plasma samples were centrifuged at 3,000 rpm for 10 minutes at 4°C, then the supernatant was collected and diluted 2-fold using the diluent provided in the Proinflammatory Panel 1 (mouse) V-PLEXTM Kit. The concentrations of IL-6 and IL-1 $\beta$  were measured using the V-PLEXTM mouse IL-6 Kit

and V-PLEXTM mouse IL-1 $\beta$  Kit on a MESO QuickPlex SQ 120 (Mesoscale Discovery, Rockville, MD) according to the manufacturers' instructions.

## Gene Expression Analysis by qRT-PCR

The relative expression levels of genes related to intestinal barrier function (*Claudin1*, *Claudin2*, *ZO-1*, and *Occludin*) in the colon were determined using qRT-PCR. Total RNA was extracted from a 1-cm-long colon segment following the cecum using the TRIzol RNA extraction method (Invitrogen, Carlsbad, CA, USA) and quantified using a NanoDrop 2,000 spectrophotometer. The total quantified RNA was then reverse transcribed to cDNA using a QuantiTect Reverse Transcription Kit (Qiagen, USA). The relative expression levels of the selected genes were determined using the ViiA<sup>TM</sup> 7 Real-Time PCR System (Applied Biosystems, USA). The Ct values of each gene were first normalized to the housekeeping gene *GAPDH* ( $\Delta$ Ct value), and the fold-change in the same gene in the control sample (mice from the CTRL group) was calculated using the  $2^{-\Delta\Delta Ct}$  method for mRNA quantification. The primer sequences for all the genes (*GAPDH*, *claudin 1*, *claudin 2*, *ZO-1*, and *occludin*) are provided in (Supplementary Table 3).

**TABLE 1** | The significantly differential compounds in FM flour vs. F-FM flour.

Name	FM (Mean $\pm$ SD)	F-FM (Mean $\pm$ SD)	Fold change	P-Value
Phosphoric acid	0.027 $\pm$ 0.0021	0.016 $\pm$ 0.0016	0.61	0.0022
Cytosine	0.0073 $\pm$ 0.00094	0.27 $\pm$ 0.021	37.40	0.0020
Hypoxanthine	0.19 $\pm$ 0.00099	0.34 $\pm$ 0.0072	1.82	<0.0001
Niacinamide	0.071 $\pm$ 0.0046	0.23 $\pm$ 0.0099	3.32	<0.0001
Adenosine	1.30 $\pm$ 0.029	0.21 $\pm$ 0.0043	0.16	0.00018
Choline	3.59 $\pm$ 0.59	8.29 $\pm$ 0.31	2.31	0.00025
D-Proline	0.71 $\pm$ 0.033	0.98 $\pm$ 0.013	1.37	0.00021
Pyrrrolidine	0.0069 $\pm$ 0.0019	0.041 $\pm$ 0.00036	5.95	<0.0001
Yuccaol C	0.15 $\pm$ 0.013	0.28 $\pm$ 0.012	1.89	0.00022
2,5-Dihydro-2,4-dimethylloxazole	0.36 $\pm$ 0.016	0.52 $\pm$ 0.083	1.44	0.032
L-Serine	0.071 $\pm$ 0.0060	0.014 $\pm$ 0.0034	0.20	0.00014
Guanine	0.16 $\pm$ 0.012	2.55 $\pm$ 0.055	16.27	<0.0001
N2,N2-Dimethylguanosine	0.0063 $\pm$ 0.00036	0.018 $\pm$ 0.00066	2.83	<0.0001
Putrescine	0.016 $\pm$ 0.00037	0.019 $\pm$ 0.00052	1.19	0.0011
6-Angeloylfuranofukinol	0.0043 $\pm$ 0.00039	0.13 $\pm$ 0.0038	31.14	0.00025
N-Methyltyramine	2.09 $\pm$ 0.17	4.32 $\pm$ 0.093	2.06	<0.0001
( $\hat{A}$ $\pm$ )-erythro-Isoleucine	1.70 $\pm$ 0.051	0.089 $\pm$ 0.0078	0.052	0.00025
ent-Epiatzelechin(2a->7,4a->8)epiatzelechin 3-(4-hydroxybenzoic acid)	0.019 $\pm$ 0.00031	0.0090 $\pm$ 0.00053	0.48	<0.0001
11-Hydroxyeicosatetraenoate glyceryl ester	0.00090 $\pm$ 0.00014	0.00015 $\pm$ 0.000065	0.17	0.0012
L-Phenylalanine	1.11 $\pm$ 0.077	0.13 $\pm$ 0.011	0.12	0.0017
2-Furancarboxaldehyde	2.09 $\pm$ 0.072	0.15 $\pm$ 0.0054	0.072	0.00042
p-Aminobenzoic acid	0.40 $\pm$ 0.0085	0.35 $\pm$ 0.015	0.86	0.0052
Prostaglandin H2 2-glyceryl Ester	0.021 $\pm$ 0.0014	0.012 $\pm$ 0.00026	0.59	0.00049
Benzyl gentiobioside	0.0010 $\pm$ 0.00016	0.00054 $\pm$ 0.000040	0.51	0.0060
L-Threonine	0.034 $\pm$ 0.0034	0.026 $\pm$ 0.0027	0.75	0.027
Guanosine	0.087 $\pm$ 0.0019	0.007 8 $\pm$ 0.00050	0.090	<0.0001
13,14-Dihydro-15-keto PGF2a	0.0034 $\pm$ 0.00036	0.0051 $\pm$ 0.00029	1.50	0.0029

## Statistics

Data sets involving more than two groups were assessed using one-way ANOVA, followed by Fisher's LSD *post hoc* tests using GraphPad Prism version 6.00 for Windows (GraphPad Software Inc., USA). A value of  $P < 0.05$  was considered to be statistically significant and presented as the mean  $\pm$  SD. A heatmap was created based on transformed z-score values using the HemI software.

## RESULTS

### Comparison of the Main Compounds of Differential Pre-treated Foxtail Millet Flours

The main compounds of Foxtail millet flours were identified using LC/MS. Comparisons with accurate mass and MS/MS data of natural products in MS2 databases revealed more than 1,000 main compounds in foxtail millet flours; In order to accurately identify more compounds influenced by different pre-treated methods, a strict filter condition was set (MS score  $> 0.99$ ; VIP  $> 1$ ). After filtering, the changes

of the main compounds across the groups were compared, and compounds that significantly changed ( $P < 0.05$ ) were listed in **Tables 1–3**.

As shown in **Tables 1–3**, when comparing the effects of differential pre-treatment methods (fermentation, germination, or both) on the main compounds in foxtail millet whole grain (F-FM vs. FM; G-FM vs. FM; FG-FM vs. FM), 27 differentially expressed compounds were identified in F-FM (compared to FM); 29 differentially expressed compounds were identified in G-FM (compared to FM); 29 differentially expressed compounds were identified in FG-FM (compared to FM). It was worth noting that 19 compounds had significant changes in all three comparisons (F-FM vs. FM; G-FM vs. FM; FG-FM vs. FM). Out of these 19 compounds, 8 of them, including Niacinamide, D-Proline, Pyrrolidine, Yuccaol C, Putrescine, N-Methyltyramine, 2-[4-(3-Hydroxypropyl)-2-methoxyphenoxy]-1,3-propanediol 1-xyloside, and Benzyl gentiobioside were up-regulated in all three pre-treated foxtail millets (F-FM, G-FM, FG-FM) when compared to un-treated foxtail millet whole grain (FM).

**TABLE 2** | The significantly differential compounds in FM flour vs. G-FM flour.

Name	FM (Mean $\pm$ SD)	G-FM (Mean $\pm$ SD)	Fold change	P-Value
Phosphoric acid	0.027 $\pm$ 0.0021	0.054 $\pm$ 0.0029	2.03	0.00018
Niacinamide	0.071 $\pm$ 0.0046	0.23 $\pm$ 0.0076	3.29	<0.0001
Adenosine	1.30 $\pm$ 0.029	1.48 $\pm$ 0.058	1.14	0.0087
Choline	3.59 $\pm$ 0.59	8.90 $\pm$ 1.70	2.48	0.0070
D-Proline	0.71 $\pm$ 0.033	5.39 $\pm$ 0.54	7.56	0.0042
Pyrrolidine	0.0069 $\pm$ 0.0019	0.22 $\pm$ 0.083	32.51	0.045
Yuccaol C	0.15 $\pm$ 0.013	0.24 $\pm$ 0.024	1.67	0.0035
2,5-Dihydro-2,4-dimethylloxazole	0.36 $\pm$ 0.016	0.53 $\pm$ 0.10	1.47	0.044
L-Serine	0.071 $\pm$ 0.0060	0.24 $\pm$ 0.046	3.47	0.021
N2,N2-Dimethylguanosine	0.0063 $\pm$ 0.00036	0.0019 $\pm$ 0.00064	0.30	0.00049
Avocadyne	0.022 $\pm$ 0.00029	0.013 $\pm$ 0.000081	5.67	<0.0001
2-Pyrrolidinone	0.051 $\pm$ 0.0021	0.060 $\pm$ 0.0052	1.18	0.044
Putrescine	0.016 $\pm$ 0.00037	0.10 $\pm$ 0.021	6.38	0.020
6-Angeloylfuranofukinol	0.0043 $\pm$ 0.00039	0.012 $\pm$ 0.00055	2.71	<0.0001
N-Methyltyramine	2.09 $\pm$ 0.17	4.09 $\pm$ 0.063	1.95	<0.0001
( $\hat{A}$ $\pm$ )-erythro-Isoleucine	1.70 $\pm$ 0.051	18.47 $\pm$ 1.69	10.85	0.0034
ent-Epiafzelechin(2a->7,4a->8)epiafzelechin 3-(4-hydroxybenzoic acid)	0.019 $\pm$ 0.00031	0.0092 $\pm$ 0.0025	0.49	0.021
2-[4-(3-Hydroxypropyl)-2-methoxyphenoxy]-1,3-propanediol 1-xyloside	0.0012 $\pm$ 0.00011	0.0016 $\pm$ 0.00013	1.41	0.0084
11-Hydroxyeicosatetraenoate glyceryl ester	0.00090 $\pm$ 0.00014	0.0063 $\pm$ 0.00060	7.06	0.00011
Quinoline	0.0079 $\pm$ 0.0011	0.033 $\pm$ 0.0020	4.21	<0.0001
Oxolan-3-one	0.043 $\pm$ 0.0023	0.050 $\pm$ 0.00082	1.16	0.0071
L-Phenylalanine	1.11 $\pm$ 0.077	14.44 $\pm$ 0.44	13.01	<0.0001
2-Furancarboxaldehyde	2.09 $\pm$ 0.072	3.59 $\pm$ 0.31	1.72	0.0012
Maltotetraose	0.00056 $\pm$ 0.00012	0.0025 $\pm$ 0.000031	4.53	0.00050
Piperidine	0.016 $\pm$ 0.0018	0.023 $\pm$ 0.0020	1.45	0.010
Benzyl gentiobioside	0.0010 $\pm$ 0.00016	0.046 $\pm$ 0.0048	43.46	0.0038
L-Threonine	0.034 $\pm$ 0.0034	0.46 $\pm$ 0.042	13.48	0.0031
Guanosine	0.087 $\pm$ 0.0019	0.17 $\pm$ 0.0038	1.91	<0.0001
13,14-Dihydro-15-keto PGF2a	0.0034 $\pm$ 0.00036	0.0016 $\pm$ 0.00011	0.48	0.0012

**TABLE 3** | The significantly differential compounds in FM flour vs. FG-FM flour.

Name	FM (Mean ± SD)	FG-FM (Mean ± SD)	Fold change	P-Value
Phosphoric acid	0.027 ± 0.0021	0.12 ± 0.0058	4.41	<0.0001
Cytosine	0.0073 ± 0.00094	0.63 ± 0.030	87.18	0.00078
Hypoxanthine	0.19 ± 0.00099	1.12 ± 0.016	5.95	<0.0001
Niacinamide	0.071 ± 0.0046	0.55 ± 0.010	7.75	<0.0001
Adenosine	1.30 ± 0.029	0.50 ± 0.014	0.38	<0.0001
Thiamine	0.086 ± 0.027	0.036 ± 0.0025	0.42	0.088
Etonogestrel	0.0042 ± 0.00069	0.019 ± 0.0011	4.55	<0.0001
D-Proline	0.71 ± 0.033	6.46 ± 0.27	9.07	0.00064
Pyrrrolidine	0.0069 ± 0.0019	0.22 ± 0.054	31.50	0.021
Yuccaol C	0.15 ± 0.013	0.35 ± 0.092	2.43	0.056
L-Serine	0.071 ± 0.0060	0.0012 ± 0.00031	0.017	0.0024
Guanine	0.16 ± 0.012	6.81 ± 0.18	43.46	0.00024
N2,N2-Dimethylguanosine	0.0063 ± 0.00036	0.020 ± 0.00074	3.13	<0.0001
Avocadyne	0.022 ± 0.00029	0.0093 ± 0.00078	4.12	0.00013
Putrescine	0.016 ± 0.00037	0.070 ± 0.014	4.35	0.021
6-Angeloylfuranofukinol	0.0043 ± 0.00039	0.093 ± 0.0024	21.54	0.00018
N-Methyltyramine	2.09 ± 0.17	5.17 ± 0.097	2.47	<0.0001
( $\Delta^{\pm}$ )-erythro-Isoleucine	1.70 ± 0.051	8.24 ± 0.66	4.84	0.0033
ent-Epiatzelechin(2a->7,4a->8)epiatzelechin 3-(4-hydroxybenzoic acid)	0.019 ± 0.00031	0.0014 ± 0.00036	0.074	<0.0001
2-[4-(3-Hydroxypropyl)-2-methoxyphenoxy]-1,3-propanediol 1-xyloside	0.0012 ± 0.00011	0.0015 ± 0.000083	1.30	0.012
Quinoline	0.0079 ± 0.0011	0.020 ± 0.0014	2.58	0.00027
L-Phenylalanine	1.11 ± 0.077	5.18 ± 0.12	4.67	<0.0001
2-Furancarboxaldehyde	2.09 ± 0.072	4.08 ± 0.20	1.96	<0.0001
Maltotetraose	0.00056 ± 0.00012	0.0085 ± 0.00035	15.10	<0.0001
Benzyl gentiobioside	0.0010 ± 0.00016	0.032 ± 0.00057	31.02	<0.0001
L-Threonine	0.034 ± 0.0034	0.083 ± 0.010	2.43	0.0015
Guanosine	0.087 ± 0.0019	0.032 ± 0.00086	0.37	<0.0001
13,14-Dihydro-15-keto PGF2a	0.0034 ± 0.00036	0.0014 ± 0.00017	0.40	0.00082
L-Valine	0.21 ± 0.0083	0.13 ± 0.0029	0.62	<0.0001

## Body Weight Loss and DAI

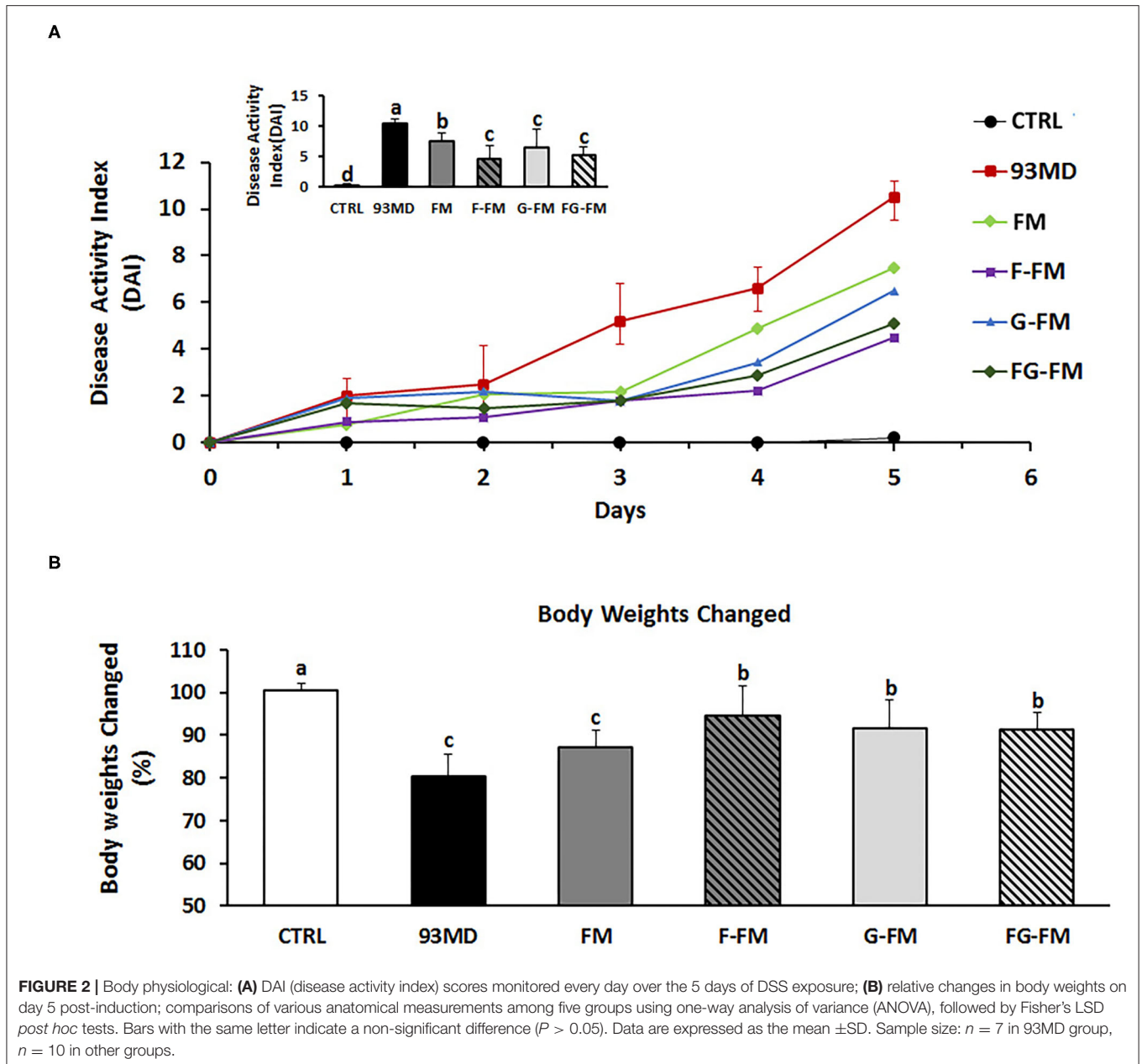
After five days of exposure to DSS, all mice exposed to DSS developed certain symptoms of enteritis in comparison to the untreated CTRL group, manifested by significant weight loss, severe diarrhea, and rectal bleeding (**Figure 2**). As shown in **Figure 2A**, disease progression in the 93MD group was obviously faster than in the foxtail millet-based diet groups. At the end of DSS induction (Day 5), mice that were fed millet-based diets had a DAI index that was significantly lower than that of the 93MD group, indicating that the four different pre-treated foxtail millet whole grains could relieve the symptoms of enteritis to varying degrees (**Figure 2A**). From a numerical point of view, the disease index of the two groups fed fermented foxtail millet diets (F-FM and FG-FM) was significantly lower compared to the mice fed unfermented foxtail millet diets (FM and G-FM), although the difference was not significant due to individual variation. In comparison to the 93MD group, the body weight loss of mice from the F-FM, G-FM, and FG-FM groups was alleviated significantly, while the body weight loss of FM showed no significant differences from that of the 93MD group (**Figure 2B**).

These results indicated that both fermentation and germination treatments were effective in alleviating body weight loss during the induction of enteritis in a mouse model.

Moreover, three of the 93MD group mice died at day 5 post-induction due to severe enteritis symptoms. DSS exposure was stopped by the end of day 5 to obtain more data, and the mice were fasted overnight and then dissected the next day. None of the mice in any other groups died during the colitis induction process.

## Pathological Characteristics and Histopathological Scores

All groups exposed to DSS displayed typical symptoms of enteritis, such as significant shortening of the colon (**Figure 3A**) and enlarged spleen (**Figure 3B**), when compared to the control group without DSS treatment. Among the groups exposed to DSS, the shortening of the colon in the 93MD group was the most significant, while in the other groups that were fed foxtail millet-based diets, it was relieved to vary degrees. The shortening



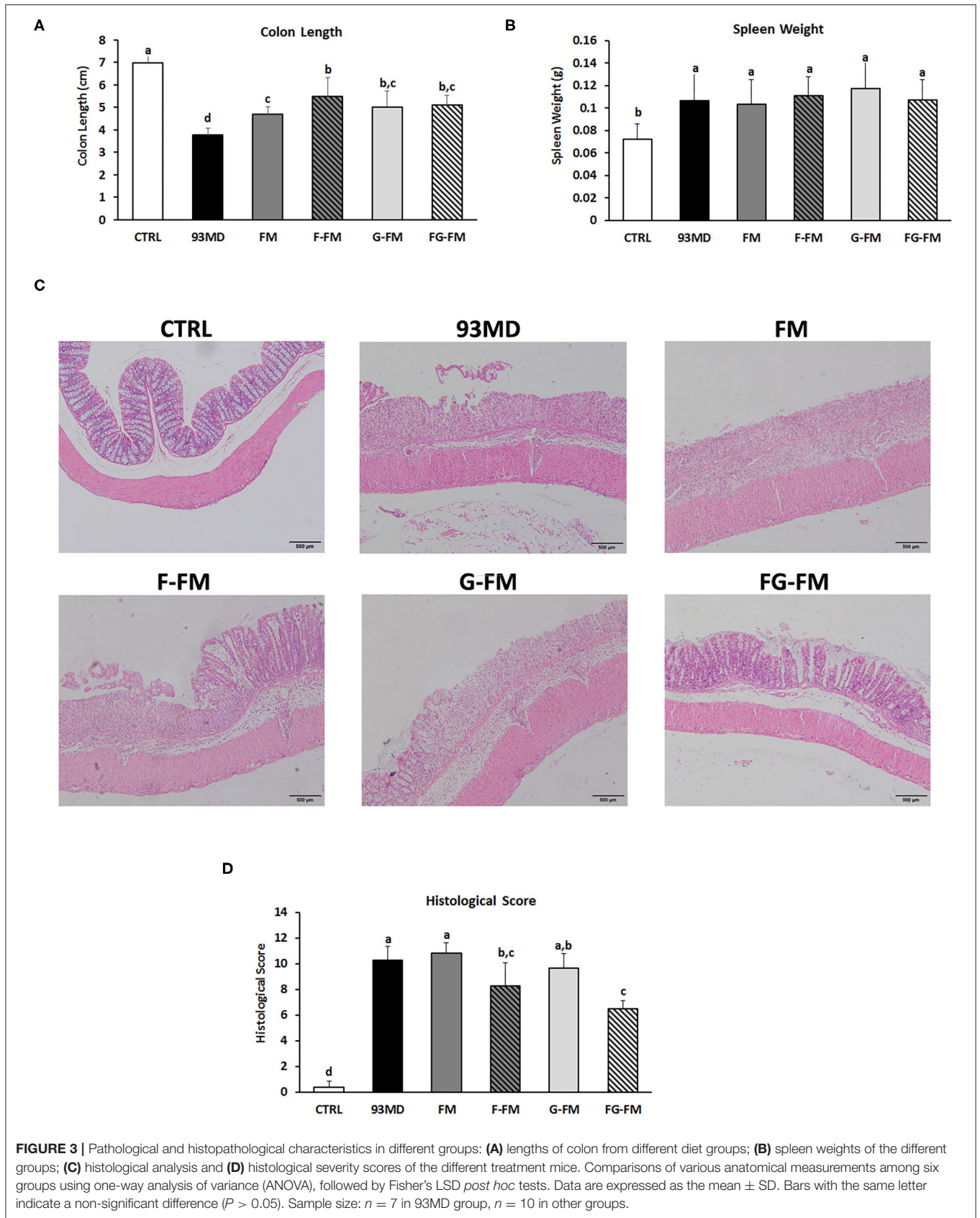
of the colon in the FM group was not relieved as well as in the other foxtail millet-based diet groups. There were no significant differences in the spleen weights of the DSS-treated groups fed different diets.

Histopathological examination (Figures 3C,D) of the colon revealed that DSS treatment induced epithelial injury in all eight DSS-treated groups. According to histopathological scores (Figure 3D), mice in the F-FM and FG-FM groups had significantly less intestinal damage than mice in the 93MD group, indicating that the fermentation process was essential to improve the ability of foxtail millet whole grains to protect mice from intestinal injury induced by DSS exposure. When combined with the histological scores of colon tissue damage, DAI, and other

indicators, it was concluded that FG-FM was more effective in preventing or alleviating symptoms of colitis.

### Gut Microbial Diversity Indices

The Chao1 index (Figure 4A) and Shannon diversity index (Figure 4B) were calculated to determine the effects of foxtail millet-based diets on the richness and diversity of bacterial species, respectively. Exposure to DSS induction significantly decreased both the Chao1 index and Shannon diversity index (CTRL vs. 93MD). The FM, F-FM, G-FM, and FG-FM groups had significantly higher Chao1 indices than the 93MD group, indicating that diets made from foxtail millet whole grains significantly restored the bacterial richness of gut microbiota.



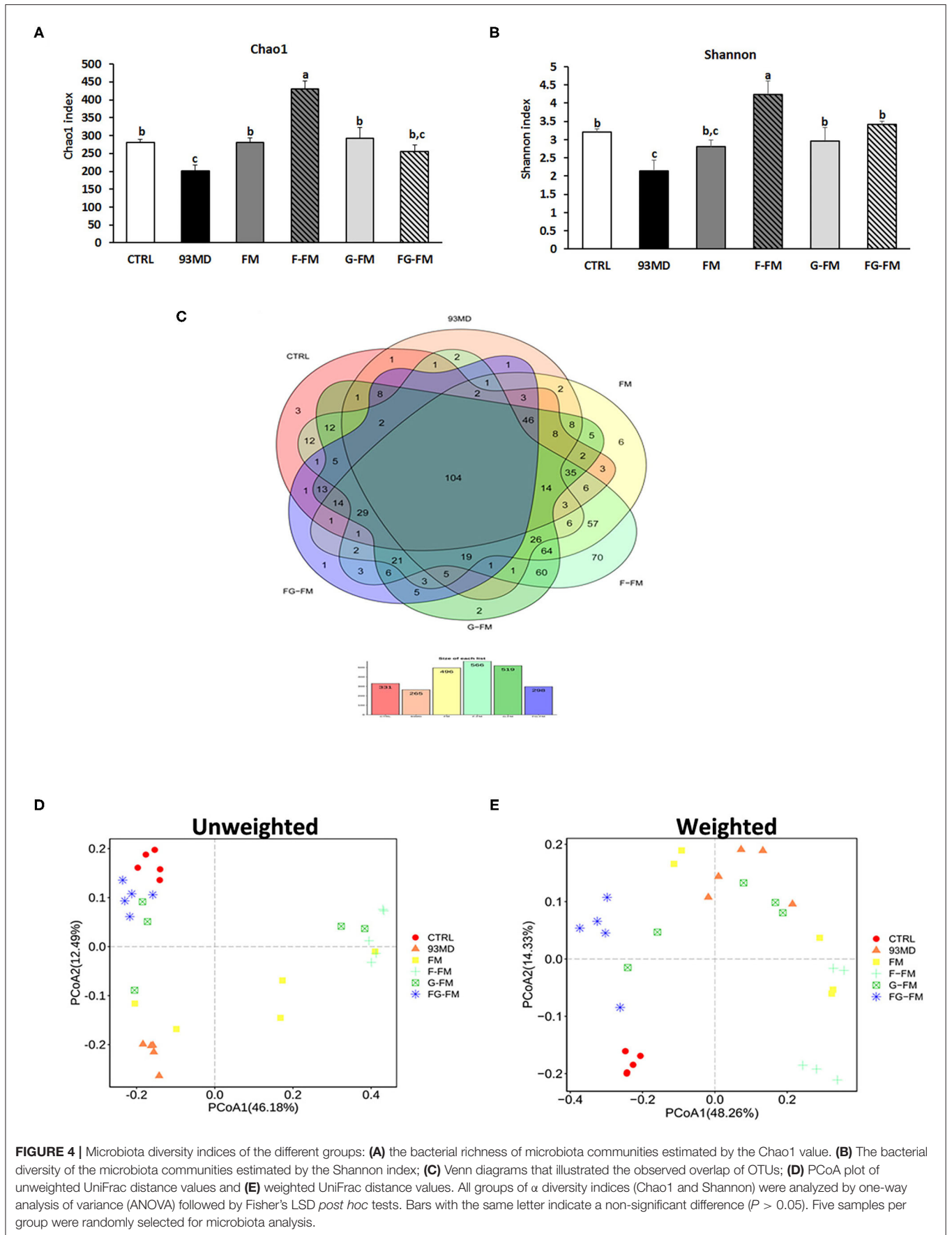


**FIGURE 4 |** Microbiota diversity indices of the different groups: **(A)** the bacterial richness of microbiota communities estimated by the Chao1 value. **(B)** The bacterial diversity of the microbiota communities estimated by the Shannon index; **(C)** Venn diagrams that illustrated the observed overlap of OTUs; **(D)** PCoA plot of unweighted UniFrac distance values and **(E)** weighted UniFrac distance values. All groups of  $\alpha$  diversity indices (Chao1 and Shannon) were analyzed by one-way analysis of variance (ANOVA) followed by Fisher's LSD *post hoc* tests. Bars with the same letter indicate a non-significant difference ( $P > 0.05$ ). Five samples per group were randomly selected for microbiota analysis.

Shannon indices were similar to Chao 1 indices in terms of details, except that the index of the FM group was not significantly higher than the 93MD group, indicating that foxtail millet whole grains pretreated by germination and fermentation had a stronger ability to restore intestinal microbial diversity than untreated foxtail millet whole grain. The shared and specific OTUs among different groups are represented by Venn diagrams in **Figure 4C**. A total of 106 OTUs were shared by all six groups, with the F-FM group having the largest number of unique OTUs (seventy). This was consistent with the results of the Chao1 and Shannon indices, which showed that the F-FM group had the highest scores. The improvement of these two indices in the foxtail millet whole grain-based diet group indicated that the foxtail millet whole grain (especially pretreated forms) had a positive effect on the intestinal flora ecosystem. There are reductions in bacterial species richness and diversity in IBD patients (40) and animal models of enteritis (33). Therefore, the promotion of microbial diversity benefits from foxtail millet whole grains may be attributed to the prevention of colitis-related symptoms.

The principal coordinates analysis (PCoA) of weighted and unweighted UniFrac distance matrix of gut microbiota is shown in **Figure 4D**, (unweighted) **Figure 4E** (weighted). In both the weighted and unweighted UniFrac plots, the CTRL group showed a significant difference from the 93MD group, as well as clear aggregation with the FG-FM group. In the unweighted UniFrac matrices, neither principal coordinate 1 (PC1, 38.48%) nor PC2 (15.27%) could separate the CTRL group from the FG-FM group; in the weighted UniFrac matrices, the CTRL and FG-FM groups did not separate in PC1 (41.81%) but were barely separated in PC2 (14.15%). This result demonstrated that intake of the FG-FM diet restored the disturbance in gut microbiota composition caused by enteritis to the greatest extent in mouse models. This positive reaction of the structure of gut microbiota communities to FG-FM diets provides important information for further research and development of functional foods for IBD.

## Composition of Gut Microbiota in Different Groups

As illustrated in **Figures 5A,B**, the composition of gut microbiota varied significantly in mice from different treatment groups. **Figure 5A** shows the significant variation in the composition of gut microbiota in mice from different groups at the phylum level. In the CTRL group, *Firmicutes* was the most dominant bacterial community (36.1%), followed by *Proteobacteria* (32.5%) and *Bacteroidetes* (22.5%). On the other hand, in the 93MD group, there was a significant reduction in the relative abundance of *Firmicutes* and *Bacteroidetes* (*Firmicutes* = 26.4%; *Bacteroidetes* = 4.1%) and a significant increase in the relative abundance of *Proteobacteria*, which were the most dominant (40.3%). This finding was consistent with the literature, which reported that the unusual expansion of *Proteobacteria* could be considered a “signature” of dysbiosis in gut microbiota (10, 41, 42). It was worth noting that in the four groups that were fed foxtail millet whole grain-based diets, the gut microbiota composition of the mice from the FG-FM group (*Firmicutes*, 51.7%; *Bacteroidetes*,

30.8%; *Proteobacteria*, 8.3%) was close to the ‘normal’ state of the CTRL group, which was also consistent with the PCoA results.

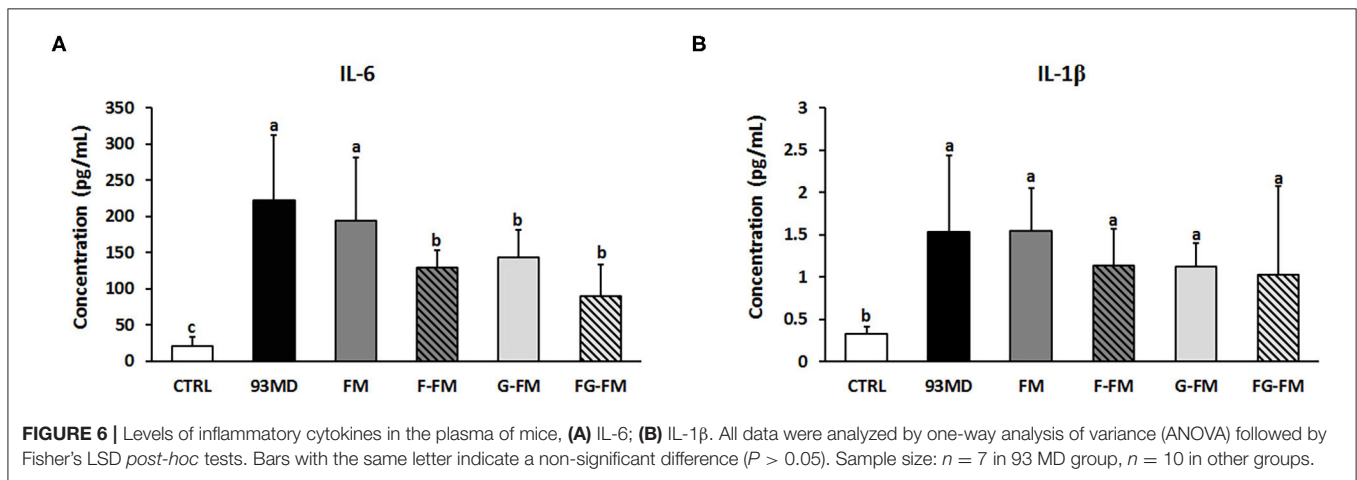
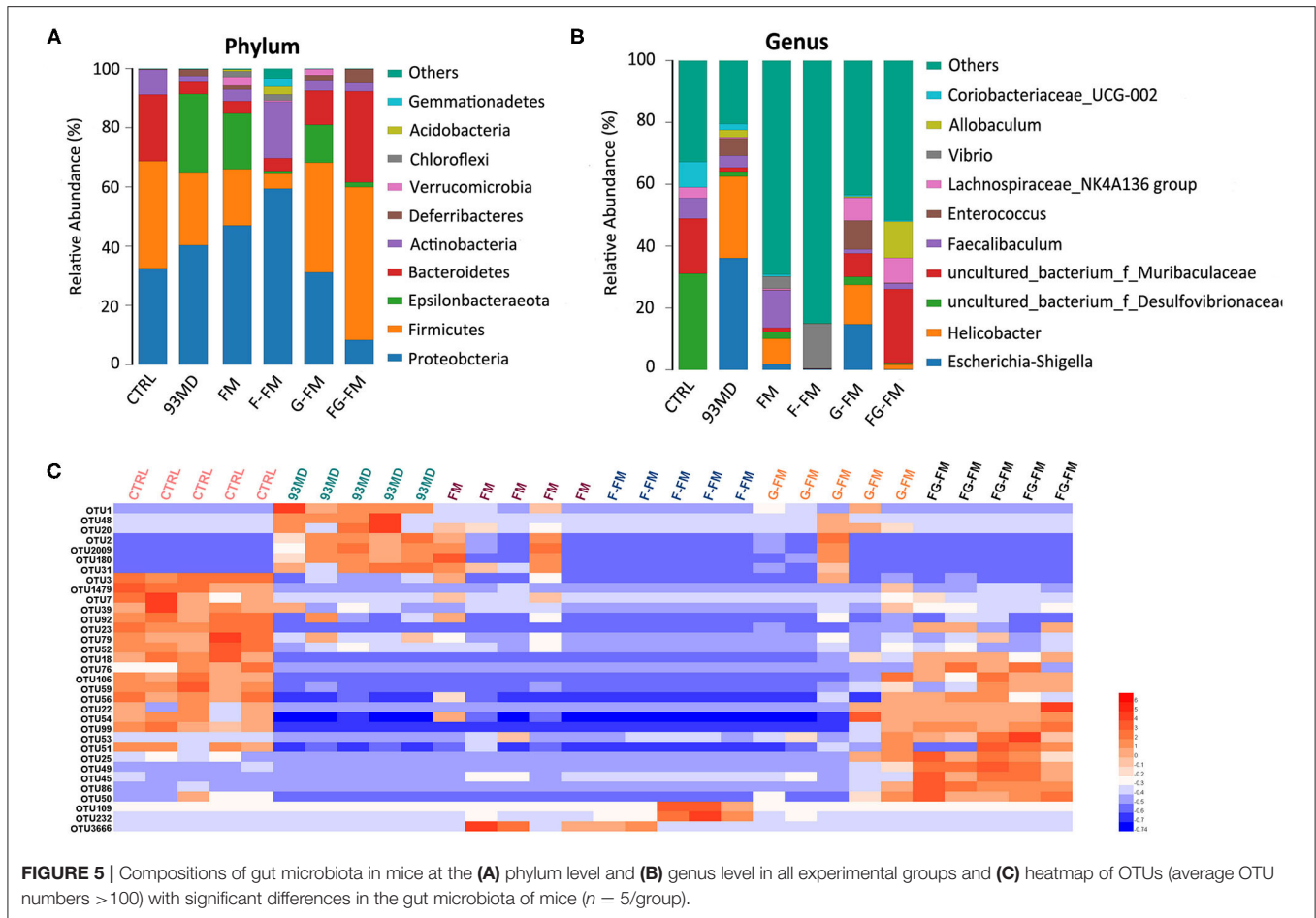
The composition analysis of the gut microbiota at the genus level (**Figure 5B**) revealed dramatic blooms of the genera *Escherichia-Shigella* and *Helicobacter* in the 93MD group (*Escherichia-Shigella*, 36.1%; *Helicobacter*, 26.4%), which were almost undetectable in the CTRL group. *Escherichia-Shigella* even occupied a predominant position in the gut microbiota of the 93MD group. However, the overexpansion of *Escherichia-Shigella* and *Helicobacter* was almost completely suppressed in the gut microbiota of mice from the F-FM and FG-FM groups.

The significant OTUs (operational taxonomic units) associated with DSS induction and diet intervention were also analyzed (**Figure 5C**). The corresponding detailed data, statistical results, and classification information are presented in **Supplementary Material**. As shown in **Figure 5C**, the numbers of OTU2, OTU1, OTU48, OTU20, OTU2009, OTU180, and OTU31 increased in the 93MD group (compared to the CTRL group), whereas the increasing trend was inhibited to varying degrees in the foxtail millet whole-grain diet groups. These OTUs were classified as uncultured bacteria from the genera OTU2 *Helicobacter* (OTU2), *Escherichia-Shigella* (OTU1), *Allobaculum* (OTU48), *Coriobacteriaceae\_UCG-002* (OTU20), *Mucispirillum* (OTU2009 and OTU180), and *Dubosiella* (OTU31). Unlike *Helicobacter* and *Escherichia-Shigella*, the genera *Allobaculum*, *Coriobacteriaceae\_UCG-002*, *Mucispirillum*, and *Dubosiella* could not be classified as either pro-inflammatory or anti-inflammatory bacteria. Taking the genus *Mucispirillum* as an example, it was identified to be associated with inflammatory bowel disease (43) or other inflammatory diseases (44), whereas it was also reported to be related to a healthier state of gut microbiota (45). These seemingly contradictory conclusions also reflect the complexity of gut microbiota structure and function.

According to **Figure 5C**, there were 16 OTUs that obviously decreased in the 93MD group compared to the CTRL group, and six of these OTUs (including OTUs 56, 22, 54, 76, 99 and 106) showed the same characteristics; that is, the numbers of these six OTUs showed an obvious rebound in the FG-FM group. These six OTUs were classified into uncultured bacterial strains from the genus *Lachnospirillum* (OTU106), genus *Desulfovibrio* (OTU22), and *Lachnospiraceae\_NK4A136* group (OTU76) and three uncultured bacterial strains from the family *Muribaculaceae* (OUT54, OTU56, and OTU99). Moreover, there were 5 OTUs significantly higher in the FG-FM group than in the other five groups, which were classified as species *Mucispirillum\_schaedleri* ASF457 (OTU25), uncultured bacteria from the genus *Lactobacillus* (OTU45), genus *Alistipes* (OTU50), and family *Muribaculaceae* (OTU49 and OTU86). Five OTUs classified to the family *Muribaculaceae* were significantly higher in the FG-FM group, which was consistent with the predominant position of *Muribaculaceae* in the gut microbiota of the FG-FM group (demonstrated in **Figure 5B**).

## Plasma Levels of Inflammatory Cytokines and Colonic Barrier Function

The levels of the inflammatory cytokines IL-6 and IL-1 $\beta$  in the plasma are shown in **Figure 6**. DSS exposure increased the



circulating levels of IL-6 and IL-1 $\beta$  compared to the untreated CTRL group. Certain foxtail millet whole grain-based diets reduced the levels of IL-6, with the FG-FM group showing the most potent anti-inflammatory effects.

As demonstrated in Table 4, the expression levels of two key tight junction proteins, *ZO-1* and *occludin*, were dramatically decreased in the DSS-induced colitis mice compared to the

CTRL group. The loss of *ZO-1* and *occludin* genes has been reported in DSS-induced colitis mouse models (46, 47). The expression of *ZO-1* and *occludin* was also below the detection level in the 93MD group. However, it was partially restored in the foxtail millet-based diet-fed mice, especially *ZO-1* in the FG-FM group. Unlike *ZO-1* and *occludin*, the expression of *claudin 1* and *claudin 2* was significantly upregulated in the majority of

**TABLE 4** | Expression levels of genes related to gut barrier function in the mouse colon.

Groups	<i>Claudin1</i>	<i>Claudin2</i>	<i>ZO-1</i>	<i>Occludin</i>
CTRL	1.00 ± 0.43 ( <b>b</b> )	1.00 ± 0.44 ( <b>b, c</b> )	1.00 ± 0.27 ( <b>a</b> )	1.00 ± 0.079 ( <b>a</b> )
93MD	10.97 ± 8.16 ( <b>a</b> )	1.53 ± 0.23 ( <b>a</b> )	ND*	ND*
FM	8.49 ± 3.31 ( <b>a</b> )	1.29 ± 0.61 ( <b>a, b</b> )	0.020 ± 0.025 ( <b>b</b> )	0.0052 ± 0.0043 ( <b>b</b> )
F-FM	7.69 ± 2.92 ( <b>a</b> )	1.19 ± 0.39 ( <b>a, b</b> )	0.29 ± 0.37 ( <b>b</b> )	0.016 ± 0.022 ( <b>b</b> )
G-FM	8.03 ± 4.62 ( <b>a</b> )	1.21 ± 0.27 ( <b>a, b</b> )	0.25 ± 0.44 ( <b>b</b> )	0.0017 ± 0.0015 ( <b>b</b> )
FG-FM	6.49 ± 2.71 ( <b>a</b> )	0.69 ± 0.12 ( <b>c</b> )	0.52 ± 0.88 ( <b>a</b> )	0.018 ± 0.011 ( <b>b</b> )

The data are expressed as the relative fold change compared to the CTRL group.

Data were expressed as Mean ± SD.

The same letter (Bold) indicates a non-significant difference ( $P > 0.05$ ).

\*Indicated below the detection limit (non-detectable).

DSS-induced colitis mice when compared to the CTRL group without DSS treatment. This observation was consistent with previous studies that reported the upregulation of *claudin 1* and *claudin 2* increased intestinal permeability and aggravated inflammation (48, 49). The intake of the FG-FM diet significantly inhibited the overexpression of *claudin2*, which also indicated the maintenance of gut barrier function in this group.

## DISCUSSION

Despite continuous efforts, the existing drugs and treatments are still not completely effective for the treatment and prevention of IBD, and pharmacological side effects of drugs are usually inevitable (50). Therefore, there is an increasing demand for the development of effective prevention strategies for IBD. Dietary strategies are very attractive in the prevention of chronic inflammation-related diseases, especially IBD, due to their low cost and safety (51). Foxtail millet is a traditional staple food in the northern areas of China and is mainly consumed as porridge. In this study, it was demonstrated that foxtail millet whole grain supplementary diets were suitable for dietary intervention in IBD. The germination or fermentation process optimized the disease suppression ability of whole-grain foxtail millet. Furthermore, whole grain foxtail millet that had undergone dual processing of germination and fermentation showed excellent anti-inflammatory properties and prebiotic characteristics, which makes it not only effective for IBD patients but also has the potential to be used as an approach to treat or prevent other intestinal diseases.

When the foxtail millet was consumed as whole grain without debranning and polishing, the fermentation process significantly enhanced its prebiotic characteristics and function to alleviate the symptoms of colitis. When consumed as a whole grain, it introduced higher dietary fiber to the diet. Although dietary fibers have been reported to possess clinical benefits for IBD patients (52), the untreated whole grain foxtail millet had no effect on relieving the symptoms of colitis in this study. However, whole grain foxtail millet that had been germinated or fermented, especially those that had undergone both the germination and fermentation processes (FG-FM group), could relieve the symptoms of enteritis to varying degrees.

The analysis of compounds in different pre-treated foxtail millet could also partially explain why the fermentation or germination process could significantly improve colitis symptoms relief and its prebiotic abilities. Despite the availability of various compounds and that most of them have not been extensively studied, the relationships between several compounds and IBD have been established. For example, nicotinamide, which was up-regulated via both fermentation and germination process, have been proved to contribute to the amelioration of experimental colitis (53). A similar case is the compound N-methyltyramine (54), although there is no direct evidence to prove its beneficial effect on IBD, a recent study has begun to focus on its role in intestinal health. Due to the complexity of the changes in the chemical composition of foxtail millet whole grain caused by fermentation or germination, the more attention should focus on this area.

The FG-FM flour displayed excellent prebiotic characteristics, including restoration of the overall composition of the intestinal flora to near-normal levels, inhibition of the proliferation of the conditional pathogenic bacteria, and promotion of beneficial bacteria growth. Although the underlying mechanism is far to be fully understood, there is no doubt that the gut microbiota plays a vital role in the pathogenesis and development of IBD (6, 10). This can also explain why FG-FM was effective in relieving the symptoms of colitis to a certain extent. For instance, *Escherichia-Shigella*, which was prevalent in the IBD patients (55), and also had higher relative abundance in the DSS-induced colitis model (56), was almost completely suppressed in the FG-WFM diet-fed mice. The predominant position of *Muribaculaceae* in the gut microbiota of the FG-FM group was also observed. In most studies, *Muribaculaceae* (also known as S24-7 clade or *Candidatus Homeothermaceae*) was significantly decreased in disease models (such as obesity, diabetes, and intestinal colitis) and rebounded following effective treatment or dietary intervention (57–59). Therefore, an increase in *Muribaculaceae* should be considered as a marker of the recovery of gut microbiota. In addition, the growth stimulation of probiotics, such as *Lactobacillus* (56), may be associated with the alleviation of colitis symptoms in the FG-FM group. This evidence indicated that the prebiotic characteristics of FG-FM might contribute to the alleviation of the symptoms of colitis in mouse models.

The foxtail millet whole grain-based diet (FG-FM) also displayed efficient anti-inflammatory activity in DSS-induced colitis mouse models. The rebalancing ability of FG-FM on gut microbiota contributed to its excellent anti-inflammatory activity based on the reported role of gut microbiota in inflammation (6). Functional loss of the gut barrier and a decrease in gut permeability are also characteristics of IBD. The upregulation of *ZO-1* and *occludin* expressions, as well as the downregulation of *claudin 2* expression, indicated that FG-FM consumption significantly increased the function of the gut barrier. Furthermore, a study reported that IL-6 monoclonal antibody treatment using DSS-induced colitis mouse models effectively suppressed the expression of *claudin 2* and attenuated gut permeability (60). This finding suggested that in FG-FM diet-fed mice, a decrease in inflammatory cytokine levels is correlated with an improved gut barrier function.

In summary, this study demonstrated that the foxtail millet supplementary diets are suitable for dietary intervention in IBD patients based on a mouse model. The germination or fermentation process optimizes the disease suppression ability of whole-grain foxtail millet. Moreover, whole grain foxtail millet that has undergone dual processing of germination and fermentation had excellent pro-inflammatory activity and prebiotic characteristics, making it effective not only for IBD patients but also for the treatment or prevention of other intestinal diseases.

## DATA AVAILABILITY STATEMENT

The datasets presented in this study can be found in online repositories. The names of the repository/repositories and

accession number(s) can be found below: <https://www.ncbi.nlm.nih.gov/>, PRJNA719303.

## ETHICS STATEMENT

The animal study was reviewed and approved by Ethics Committee of the Institute of Agro-food Science and Technology at Shandong Academy of Agricultural Sciences (Jinan, Shandong, China).

## AUTHOR CONTRIBUTIONS

WL: conceptualization, supervision, formal analysis, writing-original draft, and writing-review and editing. LL: conceptualization and writing-review and editing. YZ: investigation and writing-original draft preparation. DZ: supervision and investigation. XW: investigation. YY: resources. All authors contributed to the article and approved the submitted version.

## FUNDING

This study was supported by the Key Research and Development Plan of Shandong Province (Grant Number: 2018YYSP010), the Special Foundation for Taishan Scholars (Grant Number: tsqn20161067), and the Key Project of Yunnan Provincial Agricultural Union (Grant Number: 2017FG001-015).

## SUPPLEMENTARY MATERIAL

The Supplementary Material for this article can be found online at: <https://www.frontiersin.org/articles/10.3389/fnut.2021.694936/full#supplementary-material>

## REFERENCES

- Ni J, Wu GD, Albenberg L, Tomov VT. Gut microbiota and IBD: causation or correlation? *Nat Rev Gastroenterol Hepatol.* (2017) 14:573–84. doi: 10.1038/nrgastro.2017.88
- Rhodes JM, Campbell BJ. Inflammation and colorectal cancer: IBD-associated and sporadic cancer compared. *Trends Mol Med.* (2002) 8:10–6. doi: 10.1016/S1471-4914(01)02194-3
- Ng SC, Shi HY, Hamidi N, Underwood FE, Tang W, Benchimol EI, et al. Worldwide incidence and prevalence of inflammatory bowel disease in the 21st century: a systematic review of population-based studies. *Lancet.* (2018) 390:2769–78. doi: 10.1016/S0140-6736(17)32448-0
- Nishida A, Inoue R, Inatomi O, Bamba S, Naito Y, Andoh A. Gut microbiota in the pathogenesis of inflammatory bowel disease. *Clin J Gastroenterol.* (2018) 11:1–10. doi: 10.1007/s12328-017-0813-5
- Guan Q. A comprehensive review and update on the pathogenesis of inflammatory bowel disease. *J Immunol Res.* (2019) 2019:7247238. doi: 10.1155/2019/7247238
- Yu LC. Microbiota dysbiosis and barrier dysfunction in inflammatory bowel disease and colorectal cancers: exploring a common ground hypothesis. *J Biomed Sci.* (2018) 25:79. doi: 10.1186/s12929-018-0483-8
- Rowland I, Gibson G, Heinken A, Scott K, Swann J, Thiele I, et al. Gut microbiota functions: metabolism of nutrients and other food components. *Eur J Nutr.* (2018) 57:1–24. doi: 10.1007/s00394-017-1445-8
- Nagalingam NA, Kao JY, Young VB. Microbial ecology of the murine gut associated with the development of dextran sodium sulfate-induced colitis. *Inflamm Bowel Dis.* (2011) 17:917–26. doi: 10.1002/ibd.21462
- Mukhopadhyay I, Hansen R, El-Omar EM, Hold GL. IBD-what role do Proteobacteria play? *Nat Rev Gastroenterol Hepatol.* (2012) 9:219–30. doi: 10.1038/nrgastro.2012.14
- Palmela C, Chevarin C, Xu Z, Torres J, Sevrin G, Hirten R, et al. Adherent-invasive *Escherichia coli* in inflammatory bowel disease. *Gut.* (2018) 67:574–87. doi: 10.1136/gutjnl-2017-314903
- Frank DN, St Amand AL, Feldman RA, Boedeker EC, Harpaz N, Pace NR. Molecular-phylogenetic characterization of microbial community imbalances in human inflammatory bowel diseases. *Proc Natl Acad Sci USA.* (2007) 104:13780–5. doi: 10.1073/pnas.0706625104
- You JHS, Jiang X, Lee WH, Chan PKS, Ng SC. Cost-effectiveness analysis of fecal microbiota transplantation for recurrent *Clostridium difficile* infection in patients with inflammatory bowel disease. *J Gastroenterol Hepatol.* (2020) 35:1515–23. doi: 10.1111/jgh.15002
- DuPont HL, Jiang ZD, DuPont AW, Utay NS. Abnormal intestinal microbiome in medical disorders and potential reversibility by fecal microbiota transplantation. *Dig Dis Sci.* (2020) 65:741–56. doi: 10.1007/s10620-020-06102-y

14. Isaacs K, Herfarth H. Role of probiotic therapy in IBD. *Inflamm Bowel Dis.* (2008) 14:1597–605. doi: 10.1002/ibd.20465
15. Bibbo S, Ianiro G, Giorgio V, Scaldaferrri F, Masucci L, Gasbarrini A, et al. The role of diet on gut microbiota composition. *Eur Rev Med Pharmacol Sci.* (2016) 20:4742–9.
16. Santino A, Scarano A, De Santis S, De Benedictis M, Giovinazzo G, Chieppa M. Gut microbiota modulation and anti-inflammatory properties of dietary polyphenols in IBD: new and consolidated perspectives. *Curr Pharm Des.* (2017) 23:2344–51. doi: 10.2174/1381612823666170207145420
17. Obih C, Wahbeh G, Lee D, Braly K, Giefer M, Shaffer ML, et al. Specific carbohydrate diet for pediatric inflammatory bowel disease in clinical practice within an academic IBD center. *Nutrition.* (2016) 32:418–25. doi: 10.1016/j.nut.2015.08.025
18. Chen J, Duan W, Ren X, Wang C, Pan Z, Diao X, et al. Effect of foxtail millet protein hydrolysates on lowering blood pressure in spontaneously hypertensive rats. *Eur J Nutr.* (2017) 56:2129–38. doi: 10.1007/s00394-016-1252-7
19. Verma S, Srivastava S, Tiwari N. Comparative study on nutritional and sensory quality of barnyard and foxtail millet food products with traditional rice products. *J Food Sci Technol.* (2015) 52:5147–55. doi: 10.1007/s13197-014-1617-y
20. Kam J, Puranik S, Yadav R, Manwaring HR, Pierre S, Srivastava RK, et al. Dietary interventions for type 2 diabetes: how millet comes to help. *Front Plant Sci.* (2016) 7:1454. doi: 10.3389/fpls.2016.01454
21. Liu F, Shan S, Li H, Li Z. Treatment of peroxidase derived from foxtail millet bran attenuates atherosclerosis by inhibition of CD36 and STAT3 *in Vitro* and *in Vivo*. *J Agric Food Chem.* (2020) 68:1276–85. doi: 10.1021/acs.jafc.9b06963
22. Dong JL, Wang L, Lu J, Zhu YY, Shen RL. Structural, antioxidant and adsorption properties of dietary fiber from foxtail millet (*Setaria italica*) bran. *J Sci Food Agric.* (2019) 99:3886–94. doi: 10.1002/jsfa.9611
23. Yang R, Shan S, Zhang C, Shi J, Li H, Li Z. Inhibitory effects of bound polyphenol from foxtail millet bran on colitis-associated carcinogenesis by the restoration of gut microbiota in a mice model. *J Agric Food Chem.* (2020) 68:3506–17. doi: 10.1021/acs.jafc.0c00370
24. Shan S, Wu C, Shi J, Zhang X, Niu J, Li H, et al. Inhibitory effects of peroxidase from foxtail millet bran on colitis-associated colorectal carcinogenesis by the blockage of glycerophospholipid metabolism. *J Agric Food Chem.* (2020) 68:8295–307. doi: 10.1021/acs.jafc.0c03257
25. Kumar A, Henderson A, Forster GM, Goodyear AW, Weir TL, Leach JE, et al. Dietary rice bran promotes resistance to *Salmonella enterica* serovar Typhimurium colonization in mice. *BMC Microbiol.* (2012) 12:71. doi: 10.1186/1471-2180-12-71
26. Chu J, Zhao H, Lu Z, Lu F, Bie X, Zhang C. Improved physicochemical and functional properties of dietary fiber from millet bran fermented by *Bacillus natto*. *Food Chem.* (2019) 294:79–86. doi: 10.1016/j.foodchem.2019.05.035
27. Sharma N, Alam T, Goyal SK, Fatma S, Pathania S, Niranjana K. Effect of different storage conditions on analytical and sensory quality of thermally processed, milk-based germinated foxtail millet porridge. *J Food Sci.* (2018) 83:3076–84. doi: 10.1111/1750-3841.14371
28. Sharma S, Saxena DC, Riar CS. Changes in the GABA and polyphenols contents of foxtail millet on germination and their relationship with *in vitro* antioxidant activity. *Food Chem.* (2018) 245:863–70. doi: 10.1016/j.foodchem.2017.11.093
29. Pranotoa Y, Anggrahinia S, Efendib Z. Effect of natural and *Lactobacillus plantarum* fermentation on *in-vitro* protein and starch digestibilities of sorghum flour. *Food Biosci.* (2013) 2:46–52. doi: 10.1016/j.fbio.2013.04.001
30. Suma PF, Urooj A. Influence of germination on bioaccessible iron and calcium in pearl millet (*Pennisetum typhoides*). *J Food Sci Technol.* (2014) 51:976–81. doi: 10.1007/s13197-011-0585-8
31. Doppler M, Kluger B, Bueschl C, Schneider C, Krska R, Delcambre S, et al. Stable isotope-assisted evaluation of different extraction solvents for untargeted metabolomics of plants. *Int J Mol Sci.* (2016) 17. doi: 10.3390/ijms17071017
32. Xiao HT, Lin CY, Ho DH, Peng J, Chen Y, Tsang SW, et al. Inhibitory effect of the gallotannin corilagin on dextran sulfate sodium-induced murine ulcerative colitis. *J Nat Prod.* (2013) 76:2120–5. doi: 10.1021/np4006772
33. Liu W, Zhang Y, Qiu B, Fan S, Ding H, Liu Z. Quinoa whole grain diet compromises the changes of gut microbiota and colonic colitis induced by dextran Sulfate sodium in C57BL/6 mice. *Sci Rep.* (2018) 8:14916. doi: 10.1038/s41598-018-33092-9
34. Katakura K, Lee J, Rachmilewitz D, Li G, Eckmann L, Raz E. Toll-like receptor 9-induced type I IFN protects mice from experimental colitis. *J Clin Invest.* (2005) 115:695–702. doi: 10.1172/JCI22996
35. Magoc T, Salzberg SL. FLASH: fast length adjustment of short reads to improve genome assemblies. *Bioinformatics.* (2011) 27:2957–63. doi: 10.1093/bioinformatics/btr507
36. Bolger AM, Lohse M, Usadel B. Trimmomatic: a flexible trimmer for Illumina sequence data. *Bioinformatics.* (2014) 30:2114–20. doi: 10.1093/bioinformatics/btu170
37. Edgar RC, Haas BJ, Clemente JC, Quince C, Knight R. UCHIME improves sensitivity and speed of chimera detection. *Bioinformatics.* (2011) 27:2194–200. doi: 10.1093/bioinformatics/btr381
38. Edgar RC. Search and clustering orders of magnitude faster than BLAST. *Bioinformatics.* (2010) 26:2460–1. doi: 10.1093/bioinformatics/btq461
39. Quast C, Pruesse E, Yilmaz P, Gerken J, Schweer T, Yarza P, et al. The SILVA ribosomal RNA gene database project: improved data processing and web-based tools. *Nucleic Acids Res.* (2013) 41:D590–6. doi: 10.1093/nar/gks1219
40. Pascal V, Pozuelo M, Borrueal N, Casellas F, Campos D, Santiago A, et al. A microbial signature for Crohn's disease. *Gut.* (2017) 66:813–22. doi: 10.1136/gutjnl-2016-313235
41. Humbel F, Rieder JH, Franc Y, Juillerat P, Scharl M, Misselwitz B, et al. Association of alterations in intestinal microbiota with impaired psychological function in patients with inflammatory bowel diseases in remission. *Clin Gastroenterol Hepatol.* (2019) 18:2019–29. doi: 10.1016/j.cgh.2019.09.022
42. Dheer R, Davies JM, Quintero MA, Damas OM, Deshpande AR, Kerman DH, et al. Microbial signatures and innate immune gene expression in lamina propria phagocytes of inflammatory bowel disease patients. *Cell Mol Gastroenterol Hepatol.* (2019) 9:387–402. doi: 10.1016/j.jcmgh.2019.10.013
43. Shao X, Sun C, Tang X, Zhang X, Han D, Liang S, et al. Anti-inflammatory and intestinal microbiota modulation properties of jinxiang garlic (*Allium sativum* L.) polysaccharides toward dextran sodium sulfate-induced colitis. *J Agric Food Chem.* (2020) 68:12295–309. doi: 10.1021/acs.jafc.0c04773
44. Zhang X, Coker OO, Chu ES, Fu K, Lau HCH, Wang YX, et al. Dietary cholesterol drives fatty liver-associated liver cancer by modulating gut microbiota and metabolites. *Gut.* (2020) 70:761–74. doi: 10.1136/gutjnl-2019-319664
45. Kong H, Yu L, Gu Z, Li C, Ban X, Cheng L, et al. Novel short-clustered maltodextrin as a dietary starch substitute attenuates metabolic dysregulation and restructures gut microbiota in db/db mice. *J Agric Food Chem.* (2020) 68:12400–12. doi: 10.1021/acs.jafc.0c05798
46. Poritz LS, Garver KI, Green C, Fitzpatrick L, Ruggiero F, Koltun WA. Loss of the tight junction protein ZO-1 in dextran sulfate sodium induced colitis. *J Surg Res.* (2007) 140:12–9. doi: 10.1016/j.jss.2006.07.050
47. Kuo WT, Shen L, Zuo L, Shashikanth N, Ong M, Wu L, et al. Inflammation-induced occludin downregulation limits epithelial apoptosis by suppressing caspase-3 expression. *Gastroenterology.* (2019) 157:1323–37. doi: 10.1053/j.gastro.2019.07.058
48. Pope JL, Bhat AA, Sharma A, Ahmad R, Krishnan M, Washington MK, et al. Claudin-1 regulates intestinal epithelial homeostasis through the modulation of Notch-signalling. *Gut.* (2014) 63:622–34. doi: 10.1136/gutjnl-2012-304241
49. Barrett KE. Claudin-2 pore causes leak that breaches the dam in intestinal inflammation. *J Clin Invest.* (2020) 130:5100–1. doi: 10.1172/JCI140528
50. Connell WR, Kamm MA, Dickson M, Balkwill AM, Ritchie JK, Lennard-Jones JE. Long-term neoplasia risk after azathioprine treatment in inflammatory bowel disease. *Lancet.* (1994) 343:1249–52. doi: 10.1016/S0140-6736(94)92150-4
51. Halmos EP, Gibson PR. Dietary management of IBD—insights and advice. *Nat Rev Gastroenterol Hepatol.* (2015) 12:133–46. doi: 10.1038/nrgastro.2015.11
52. Galvez J, Rodriguez-Cabezas ME, Zarzuelo A. Effects of dietary fiber on inflammatory bowel disease. *Mol Nutr Food Res.* (2005) 49:601–8. doi: 10.1002/mnfr.200500013
53. Bettenworth D, Nowacki TM, Ross M, Kyme P, Schwambach D, Kerstiens L, et al. Nicotinamide treatment ameliorates the course of experimental colitis

- mediated by enhanced neutrophil-specific antibacterial clearance. *Mol Nutr Food Res.* (2014) 58:1474–90. doi: 10.1002/mnfr.201300818
54. Ni J, Guo Y, Chang N, Cheng D, Yan M, Jiang M, et al. Effect of N-methyltyramine on the regulation of adrenergic receptors via enzymatic epinephrine synthesis for the treatment of gastrointestinal disorders. *Biomed Pharmacother.* (2019) 111:1393–8. doi: 10.1016/j.biopha.2018.12.145
55. Chen L, Wang W, Zhou R, Ng SC, Li J, Huang M, et al. Characteristics of fecal and mucosa-associated microbiota in Chinese patients with inflammatory bowel disease. *Medicine.* (2014) 93:e51. doi: 10.1097/MD.0000000000000051
56. Zhu X, Xiang S, Feng X, Wang H, Tian S, Xu Y, et al. Impact of cyanocobalamin and methylcobalamin on inflammatory bowel disease and the intestinal microbiota composition. *J Agric Food Chem.* (2019) 67:916–26. doi: 10.1021/acs.jafc.8b05730
57. Lagkouvardos I, Lesker TR, Hitch TCA, Galvez EJC, Smit N, Neuhaus K, et al. Sequence and cultivation study of Muribaculaceae reveals novel species, host preference, and functional potential of this yet undescribed family. *Microbiome.* (2019) 7:28. doi: 10.1186/s40168-019-0637-2
58. Chen KJ, Chen YL, Ueng SH, Hwang TL, Kuo LM, Hsieh PW. Neutrophil elastase inhibitor (MPH-966) improves intestinal mucosal damage and gut microbiota in a mouse model of 5-fluorouracil-induced intestinal mucositis. *Biomed Pharmacother.* (2021) 134:111152. doi: 10.1016/j.biopha.2020.111152
59. Li ZR, Jia RB, Wu J, Lin L, Ou ZR, Liao B, et al. Sargassum fusiforme polysaccharide partly replaces acarbose against type 2 diabetes in rats. *Int J Biol Macromol.* (2021) 170:447–58. doi: 10.1016/j.ijbiomac.2020.12.126
60. Xiao YT, Yan WH, Cao Y, Yan JK, Cai W. Neutralization of IL-6 and TNF- $\alpha$  ameliorates intestinal permeability in DSS-induced colitis. *Cytokine.* (2016) 83:189–92. doi: 10.1016/j.cyto.2016.04.012

**Conflict of Interest:** The authors declare that the research was conducted in the absence of any commercial or financial relationships that could be construed as a potential conflict of interest.

**Publisher's Note:** All claims expressed in this article are solely those of the authors and do not necessarily represent those of their affiliated organizations, or those of the publisher, the editors and the reviewers. Any product that may be evaluated in this article, or claim that may be made by its manufacturer, is not guaranteed or endorsed by the publisher.

Copyright © 2021 Zhang, Liu, Zhang, Yang, Wang and Li. This is an open-access article distributed under the terms of the Creative Commons Attribution License (CC BY). The use, distribution or reproduction in other forums is permitted, provided the original author(s) and the copyright owner(s) are credited and that the original publication in this journal is cited, in accordance with accepted academic practice. No use, distribution or reproduction is permitted which does not comply with these terms.